scientific reports

Check for updates

OPEN

Kinetic analysis of catalytic activity of G-quadruplex/hemin DNAzyme with flanking adenine nucleotides

Anuttara Udomprasert[1]✉, Sutida Chimasungkanun[2] & Thaned Kangsamaksin[2]✉

G-quadruplex/hemin DNAzymes are promising nucleic acid catalysts due to their versatility and ease of use in biosensing applications. Their peroxidase-like catalytic activity can be enhanced through various strategies, including modifications to flanking nucleotides. In this study, the catalytic effects of flanking nucleotide modifications at the 3′ and 5′ ends of the DNAzyme were investigated. Additionally, the structural topology of the G-quadruplex/hemin DNAzymes was characterized using circular dichroism (CD) spectroscopy. Similar to the unmodified DNAzyme, the modified G-quadruplex with adenine (A) nucleotide at the 3′-terminal extension adopted a parallel topology in the presence of hemin. After optimizing the reaction conditions, the kinetic parameters of both original and 3′ flanking A modified G-quadruplex/hemin DNAzymes were evaluated using the oxidation of 2,2′-azino-bis(3-ethylbenzothiazoline-6-sulfonic acid) (ABTS) in the presence of hydrogen peroxide (H_2O_2). The kinetic analysis revealed a significant enhancement in catalytic efficiency upon the addition of A nucleotides at the 3′ end. Notably, the DNAzyme with a 3′-terminal AA modification exhibited approximately a ten-fold increase in catalytic efficiency compared to the unmodified form, as indicated by higher turnover numbers (k_{cat}) and lower H_2O_2 substrate affinity (K_m). This enhanced catalytic performance was further demonstrated by improved colorimetric signal detection of circulating tumor DNA (ctDNA), underscoring the potential of the modified DNAzymes for more sensitive detection in colorimetric biosensor applications.

Keyword G-quadruplex/hemin DNAzyme, Kinetics study, Colorimetric biosensor

Nucleic acids are essential macromolecules that serve as the genetic material in all living organisms. Beyond their conventional genetic roles, certain nucleic acids—referred to as functional nucleic acids—carry out specialized tasks[1]. These include aptamers, which bind specific targets similarly to antibodies, and DNAzymes (or deoxyribozymes), which exhibit catalytic activity akin to protein enzymes. DNAzymes can catalyze a variety of chemical reactions, such as the cleavage and ligation of oligonucleotides[2,3], and the oxidation of organic molecules[4,5].

Among the reported DNAzymes, G-quadruplex/hemin DNAzymes have attracted considerable attention for their applications in biological and analytical fields[6–9]. First described by Travascio and colleagues in 1998[10], these DNAzymes were identified via the systematic evolution of ligands by exponential enrichment (SELEX) method, yielding a hemin-binding DNA aptamer that exhibited peroxidase-like catalytic activity. These DNAzymes consist of a guanine (G)-rich single-stranded DNA (ssDNA) folded into a G-quadruplex structure, bound to hemin (iron(III)-protoporphyrin IX). Functionally, they mimic the activity of horseradish peroxidase (HRP), catalyzing the oxidation of organic substrates in the presence of hydrogen peroxide (H_2O_2)[11]. Various substrates can be utilized to generate detectable signals, including ABTS (2,2′-azino-bis(3-ethylbenzothiazoline-6-sulfonic acid))[10,12], TMB (3,3′,5,5′-tetramethylbenzidine sulfate)[13,14], and NADH (β-nicotinamide adenine dinucleotide)[15,16] for colorimetric detection, as well as luminol[17,18], tyramine[16,19], and Amplex Red[20,21] for fluorescence-based detection. G-quadruplex/hemin DNAzymes offer several advantages over protein enzymes, such as greater resistance to hydrolysis and heat, lower production costs, and ease of chemical modification[21,22]. However, their catalytic efficiency remains a key limitation, as it is significantly lower than that of HRP[11].

Numerous studies have sought to enhance the peroxidase-mimicking activity of G-quadruplex/hemin DNAzymes by modifying their G-rich ssDNA sequences. For example, Golub et al. developed a hybrid DNAzyme termed a "nucleoapzyme" by conjugating a G-quadruplex sequence (5′-TTTGGGTAGGGCGGGTTGGG-3′) with a DNA recognition element, resulting in improved catalytic performance[23]. Other efforts involved

[1]Department of Biochemistry, Faculty of Science, Burapha University, Chonburi 20131, Thailand. [2]Department of Biochemistry, Faculty of Science, Mahidol University, Bangkok 10400, Thailand. ✉email: anuttara@go.buu.ac.th; thaned.kan@mahidol.edu

covalently linking hemin to G-quadruplex sequences (5′-GTGGGTAGGGCGGGTTGG-3′ and 5′-TGGGTAG GGCGGGTTGGGAAA-3′), enhancing both catalytic efficiency and thermal stability[24,25]. Dimeric DNAzymes constructed from the monomeric sequence 5′-GGGTAGGGCGGGTTGGG-3′ exhibited even higher activity[26], and multimeric DNAzymes were reported to show synergistic catalytic effects exceeding the sum of individual monomers (5'-GTGGGTAGGGCGGGTTGG-3')[27]. Several additives have also been shown to enhance catalytic activity. For instance, ATP not only boosts the activity of G-quadruplex/hemin DNAzymes (5′-TGGGTAGGG CGGGTTGGGAAA-3′) but also stabilizes ABTS•+ radicals[28]. Spermine is another potent additive, significantly increasing activity for several DNAzyme sequences (5'-GTGGGTAGGGCGGGTTGG-3' and 5'-TGGGTA GGGCGGGTTGGGAAA-3')[29]. Among the many strategies explored, modifying the flanking sequences—particularly by appending adenine (A) or cytosine (C) residues to the 3′ or 5′ ends—has been extensively studied. For example, flanking G-quadruplex/hemin DNAzymes (5′-GGGTGGGTGGGTGGG-3′) with cytosine triplets (dCCC) at both ends significantly improved activity[11]. The position of the flanking nucleotides was also found to influence enhancement; placing cytosine at the second position of the 3′ end yielded the greatest activity[30]. A comprehensive study modifying each terminal position with all four nucleotides (5′-GGGTAGGGCGGGTTG GG-3′) found that only adenine at the 3′ end enhanced catalytic activity[31]. Similar improvements were observed with dA-flanked tetramolecular G-quadruplexes (5′-GGGG-3′, 5′-GGGGG-3′, and 5′-GGGGGG-3′)[32], as well as modified constructs with two identical 3′ ends on a single DNA strand[33]. Flanking both the 5′ and 3′ ends with dA (5′-GGGTGGGTGGGTGGG-3′ and 5′-AGGGGA-3′) or using G-modified bases (such as 8-bromo-2′-deoxyguanosine) also confirmed the catalytic enhancement effect of dA[16]. Additionally, repeating dA units in the loop regions of G-quadruplex structures (5′-GGGTGGG-X_n-GGGTGGG-3′) showed similar benefits[34]. While dC flanking improves activity primarily by increasing hemin binding affinity[11], dA flanking enhances activity without directly contributing to hemin binding[31,35] and does not interfere with G-quadruplex formation[30].

Despite these findings, kinetic data on modified DNAzymes remain limited. Kinetic studies are essential for understanding the fundamental catalytic behavior of DNAzymes, as they provide key parameters that describe enzyme-like function. Most previous investigations have relied primarily on velocity to demonstrate the effects of G-quadruplex/hemin DNAzyme modifications[31–34]. While velocity reflects the overall catalytic rate, other critical parameters are necessary to fully characterize catalytic behavior. These include the Michaelis–Menten constant (K_m), which represents the substrate concentration required to reach half of maximum velocity (v_{max}); the turnover number (k_{cat}), which indicates the maximum number of substrate molecules converted to product per unit time; and the catalytic efficiency (k_{cat}/K_m), which integrates catalytic rate with substrate affinity to provide a comprehensive measure of catalytic effectiveness. Such kinetic information is vital for the rational development of G-quadruplex/hemin DNAzymes with efficiencies approaching those of natural enzymes such as horseradish peroxidase (HRP). To the best of our knowledge, detailed kinetic parameters for G-quadruplex/hemin DNAzymes modified with a 3′ flanking adenine have not yet been reported.

This study aimed to investigate the kinetics behavior of the modified G-quadruplex/hemin DNAzymes with flanking adenine nucleotides. The fundamental knowledge of DNAzyme catalysis could be used to develop the modified G-quadruplex/hemin DNAzymes with higher catalytic efficiency. Many previously reported G-quadruplex/hemin DNAzymes share a common core sequence, 5′-GGGTAGGGCGGGTTGGG-3′, as shown in Figure S1 and all the DNA sequences used in this study are listed in Table S1. In this study, we selected this core sequence as a model (Fig. 1A) to investigate the effects of flanking nucleotide modifications (Fig. 1B) on catalytic performance using ABTS and H_2O_2 as substrates (Fig. 1C). The catalytic activities of unmodified and flanking-modified DNAzymes were compared. After optimizing reaction conditions, we employed circular dichroism (CD) spectroscopy to confirm G-quadruplex topology. Since the highest activity was observed with dA flanking at the 3′ end, we further conducted kinetic analyses of these modified DNAzymes. The improved catalytic activity was validated through enhanced colorimetric detection of circulating tumor DNA (ctDNA), demonstrating their potential application in sensitive biosensing platforms.

Results and discussion

Catalytic activity of G-quadruplex/hemin DNAzyme with nucleotide modifications

To investigate the effect of flanking nucleotides on the catalytic activity of G-quadruplex/hemin DNAzymes, a series of DNAzyme variants were designed by appending nucleotides (A, C, T, or G) to either the 3′ or 5′ ends of the core sequence. The catalytic activity of each variant was evaluated relative to the unmodified DNAzyme. In the catalytic reaction, ABTS serves as the electron donor, transferring electrons to H_2O_2, which results in the formation of the oxidized product ABTS•+. This green-colored product is detectable by UV–vis spectrophotometry at 420 nm. The results revealed distinct differences in catalytic activity among the modified DNAzymes. Notably, enhanced catalytic activity was observed in variants with adenine (A) and cytosine (C) modifications (Fig. 2A,B). Among these, modifications at the 3′ end consistently exhibited significantly higher catalytic activity than those at the 5′ end for both A and C. This trend may be attributed to the preferential stacking of hemin at the 3′ end, as previously suggested in the literature[31,32,36,37]. The highest catalytic activity was observed with the adenine-modified DNAzyme at the 3′ end. In contrast, modifications with thymine (T) or guanine (G) showed no improvement in catalytic performance (Fig. 2C,D). These findings are consistent with earlier reports indicating that A and C modifications enhance the activity of G-quadruplex/hemin DNAzymes, whereas T has minimal effect[30]. This difference may be explained by the distinct chemical properties of the nucleotides: adenine and cytosine possess unprotonated nitrogen atoms and exocyclic amino groups (-NH_2), which can mimic the function of the distal histidine residue in horseradish peroxidase (HRP), facilitating the formation of reactive oxidation states in the iron porphyrin core. In contrast, thymine lacks both unprotonated nitrogen and exocyclic amino groups, potentially limiting its ability to enhance catalysis. Furthermore, a single adenine modification induced a greater catalytic enhancement than a triple cytosine modification, likely due to lower G-quadruplex formation and adenine's higher electron density compared to cytosine[12]. In addition,

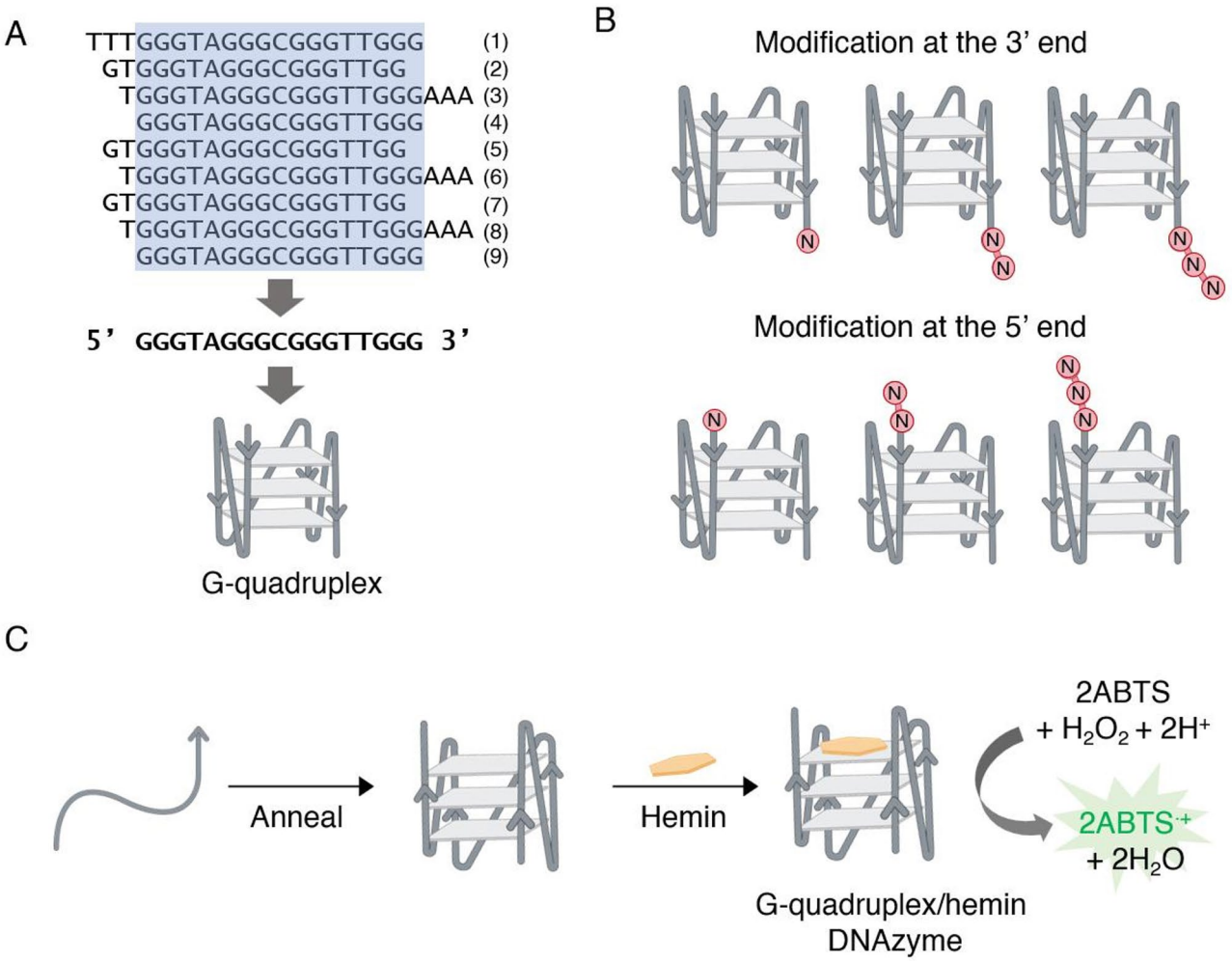

Fig. 1. Schematic of G-quadruplex/hemin DNAzyme modifications and their catalytic reaction. The core sequence of our design based on the sequence alignment of previously reported G-quadruplex/hemin DNAzymes[23–29,31] (A). G-quadruplex/hemin DNAzyme and its derivatives with flanking nucleotide modification at either 3' or 5' end (B). The G-quadruplex/hemin DNAzyme preparation and the catalytic activity of DNAzyme using ABTS and H_2O_2 as substrates (C).

the flanking nucleotide modification seems not to affect the folding of G-quadruplex structure confirmed with the CD spectra (Figure S2A–S2F) and the binding of these modified G-quadruplex structures to hemin analyzed with UV–Vis absorption spectra (Figure S2G–S2L) except for the 3' CCC modification compared with the unmodified G-quadruplex/hemin DNAzyme. However, DNAzyme 3' CCC still exhibits greater catalytic activity compared to the unmodified one. The consistently greater activity enhancement observed with 3′-end modifications, as opposed to 5′-end modifications, further supports previous findings on the positional effects of flanking nucleotides[31,32].

Optimization of experimental conditions for catalytic activity study

To optimize the experimental conditions, the DNAzyme modified with two adenine nucleotides at the 3′ end (DNAzyme 3′ AA), which demonstrated the highest catalytic activity, was selected for further investigation. Various G-rich sequences capable of forming G-quadruplex structures, as well as a range of buffer systems for activity assays, have been reported in the literature, including Tris–HCl, HEPES, and MES buffers[23–28,31]. It is well established that the formation of G-quadruplex structures requires monovalent cations such as K^+ or Na^+ for structural stabilization[38]. In line with previous studies, the G-quadruplex structure was initially annealed and incubated with hemin in Tris–HCl buffer supplemented with 50 mM K^+, and the catalytic activity was subsequently measured in 25 mM MES buffer (pH 5.1) containing 200 mM NaCl, 10 mM KCl, 1% DMSO, and 0.05% Triton X-100[31,39]. To evaluate the effect of potassium ion concentration on catalytic performance, the DNAzyme was annealed in 10 mM Tris–HCl buffer (pH 8.0) with varying concentrations of KCl (0–200 mM). Surprisingly, no significant differences in catalytic activity were observed across the tested KCl concentrations (Fig. 3A). As a result, subsequent experiments utilized DNAzymes annealed in 10 mM Tris–HCl buffer (pH 8.0) without additional KCl.

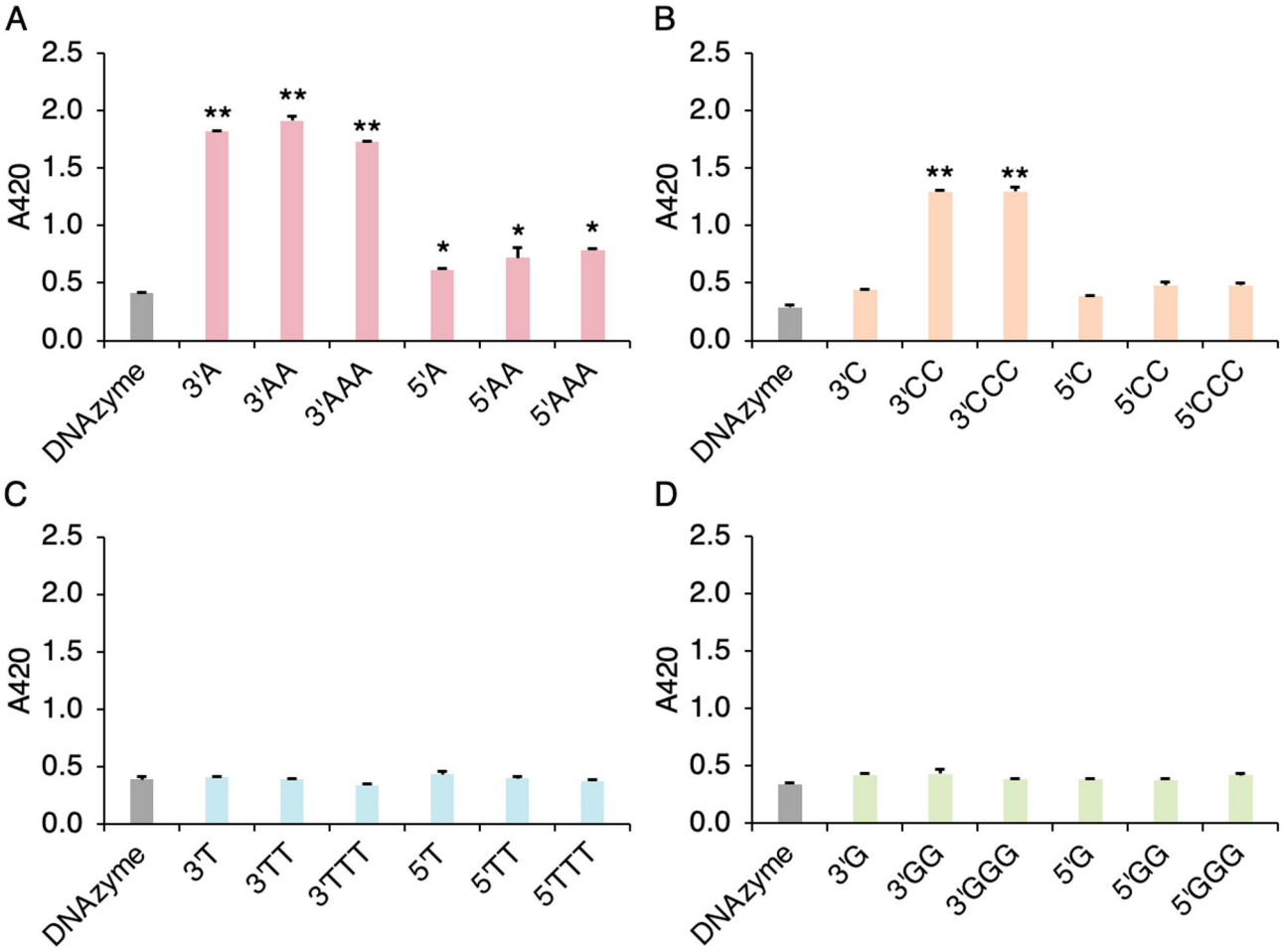

Fig. 2. Comparison of the catalytic activity of G-quadruplex/hemin DNAzymes with nucleotide modifications; DNAzyme modified with A nucleotides (**A**), C nucleotides (**B**), T nucleotides (**C**), and G nucleotides (**D**). Data presented ± S.D. * P value < 0.01, ** P value < 0.001.

It is worth noting that free hemin can independently catalyze peroxidase-like reactions, albeit at a much slower rate than the G-quadruplex/hemin complex[40]. Therefore, the effect of hemin concentration on catalytic activity was assessed. The G-quadruplex structure alone showed no catalytic activity in the absence of hemin (Fig. 3B). Activity increased with rising DNAzyme:hemin ratios, reaching a maximum at a 1:10 ratio, beyond which no further enhancement was observed—consistent with previous findings[4]. Accordingly, a 1:10 DNAzyme:hemin ratio was adopted for subsequent assays. In earlier reports, G-quadruplex structures were formed by heating the DNAzyme at 90 °C for 5 min, followed by slow cooling to room temperature over two hours, and incubation with hemin for 30 minutes[39]. To streamline this process, different cooling durations were tested. Notably, reducing the cooling time to 15 min yielded catalytic activity comparable to the standard two-hour protocol (Fig. 3C). Therefore, in subsequent preparations, hemin was added immediately after the heating step, omitting the cooling phase altogether. Finally, the optimal incubation time with hemin was determined. Maximum catalytic activity was observed with a 30-min incubation (Fig. 3D), consistent with previous findings for the unmodified DNAzyme (Figure S3). Based on these optimizations, the final preparation protocol involved annealing the DNAzyme in 10 mM Tris–HCl buffer (pH 8.0) without KCl, heating at 90 °C for 5 min, immediate addition of hemin at a 1:10 DNAzyme:hemin ratio, and incubation for 30 min. These refinements significantly reduced the preparation time while preserving robust catalytic activity, thereby enhancing experimental efficiency.

Structural characterization of G-quadruplex/hemin DNAzyme with AA nucleotide modifications

The topology of the G-quadruplex structure plays a critical role in determining the catalytic activity of G-quadruplex/hemin DNAzymes. Previous studies have shown that G-quadruplexes can adopt various conformations—parallel, antiparallel, and hybrid—with the parallel topology typically exhibiting the highest catalytic efficiency[26,41]. Circular dichroism (CD) spectroscopy is widely employed to differentiate among these conformations[25]. To evaluate the structural impact of adenine modifications at the 3′ end, the G-quadruplex topologies of the unmodified DNAzyme and the DNAzyme with 3′ AA flanking nucleotides were analyzed by CD spectroscopy in the presence and absence of hemin after annealing in Tris–HCl buffer (pH 8.0). Notably,

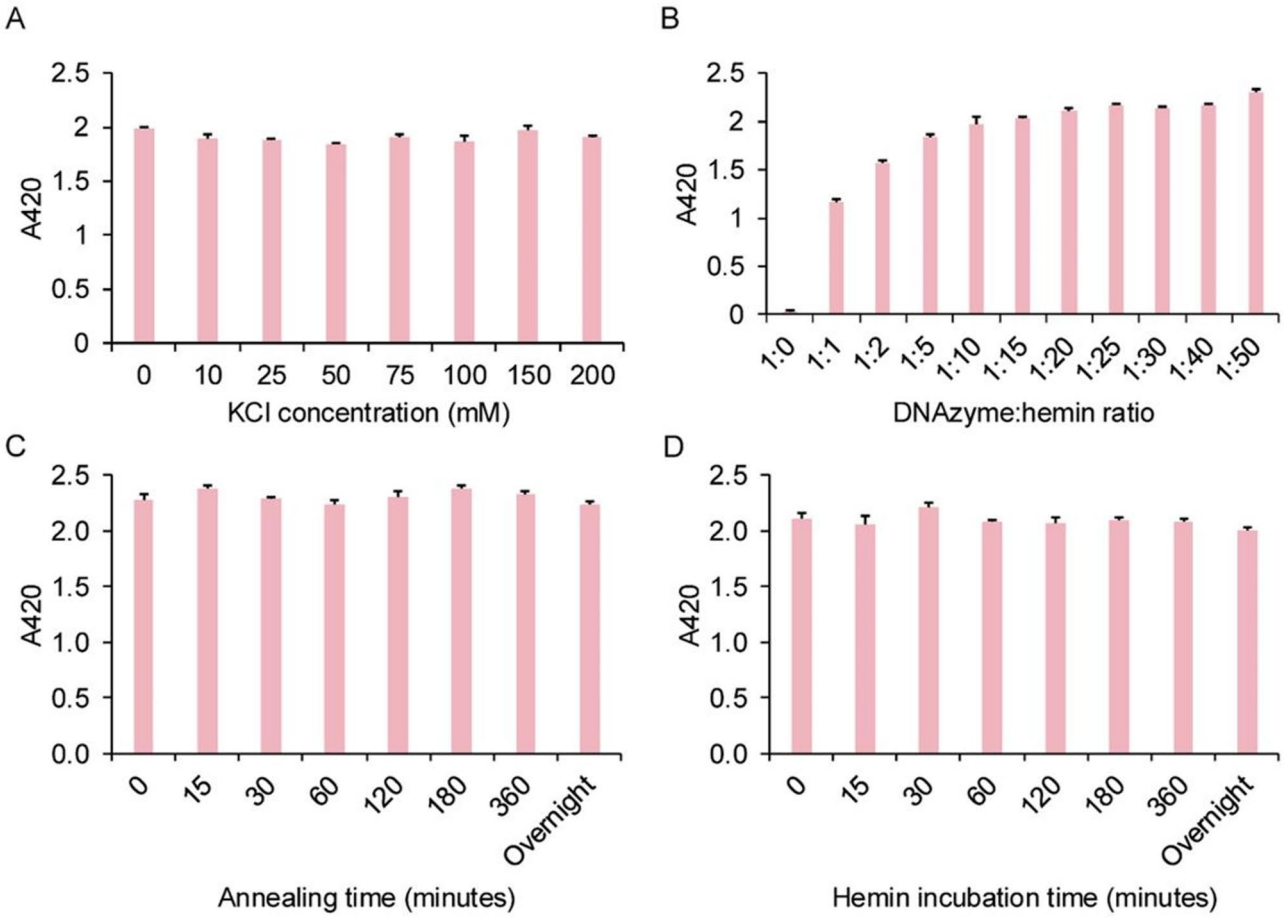

Fig. 3. The condition optimization of catalytic activity of DNAzyme with 3' AA nucleotide modifications; the KCl concentrations (**A**), the DNAzyme:hemin ratio (**B**), the cooling down period (**C**), and the hemin incubation time (**D**). Data presented ± S.D.

G-quadruplex formation was observed only in the presence of hemin, as evidenced by the appearance of characteristic CD signals. Both DNAzyme variants exhibited a negative peak around 240 nm and a positive peak around 260 nm, consistent with the spectral signature of a parallel G-quadruplex conformation (Fig. 4A,B). These findings confirm that the G-rich core sequence retains its ability to fold into a parallel G-quadruplex structure, even with 3′ AA modification, in agreement with prior reports[26,30,31,34]. Interestingly, the results also suggest that hemin alone can facilitate the folding of these sequences into a G-quadruplex structure in the absence of potassium ions, highlighting its role as a structural co-factor in K^+-free buffer conditions. However, it is important to note that CD analysis suggests the presence of K^+ ions is not essential for G-quadruplex formation when hemin is present. Annealing the G-quadruplex structure in Tris–HCl buffer, either with or without K^+, yielded comparable catalytic activities in MES buffer, which does contain K^+. These results indicate that, for potential biological applications, the presence of K^+ ions in the surrounding medium is unlikely to exert a significant influence on the catalytic activity of the G-quadruplex/hemin DNAzyme.

Kinetic study of G-quadruplex/hemin DNAzymes

The kinetic parameters of both unmodified and modified G-quadruplex/hemin DNAzymes were evaluated by monitoring the oxidation of ABTS in the presence of H_2O_2. The reaction was tracked by measuring the change in absorbance at 420 nm over time. Initial velocities (v_o) were determined for each DNAzyme (2.5 nM) across a range of ABTS concentrations (0.1–6.0 mM), while maintaining a fixed H_2O_2 concentration of 300 mM. Michaelis–Menten plots for each DNAzyme variant are shown in Fig. 5A–D. Kinetic parameters were calculated using KaleidaGraph software based on triplicate measurements (with individual replicates shown in Figure S4), and are summarized in Fig. 5E. The results demonstrated that all modified DNAzymes exhibited a substantial increase in maximum reaction velocity (v_{max}), with approximately a 12.5-fold enhancement relative to the unmodified DNAzyme. The extent of catalytic enhancement did not vary significantly with the number of adenine residues (1 to 3) appended to the 3′ end, consistent with previous findings[31]. However, all modified DNAzymes showed higher Michaelis constants (K_m), indicating a reduced affinity for the ABTS substrate. This suggests that although A-modifications enhance catalytic turnover, they do not improve substrate binding affinity, necessitating higher ABTS concentrations to achieve v_{max}. Importantly, the turnover number (k_{cat}) for

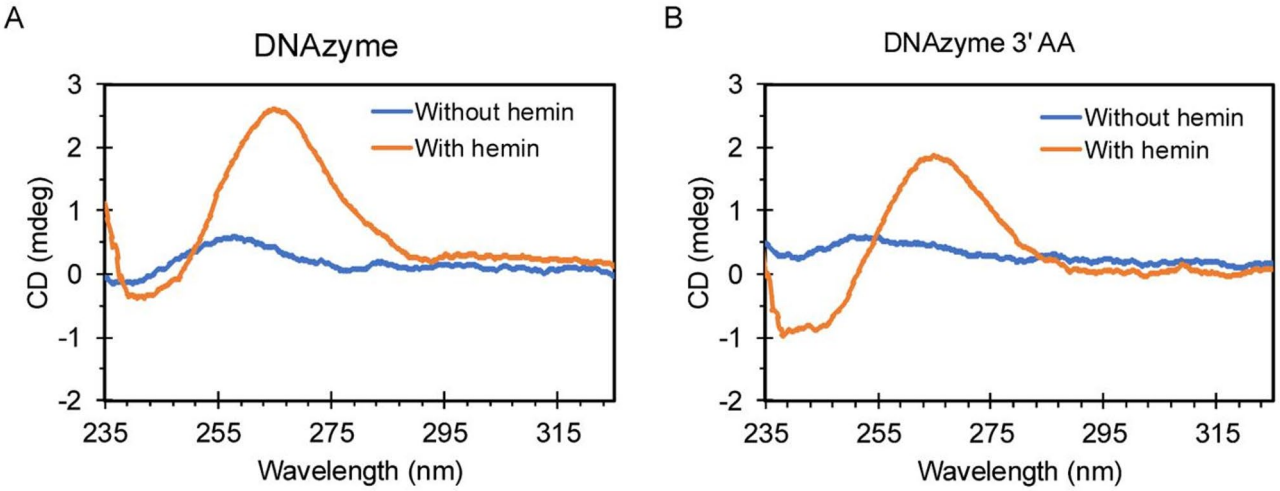

Fig. 4. CD spectra of DNAzyme (**A**) and DNAzyme with 3' AA (**B**) in the presence (orange) and absence of hemin (blue). Average data from three replicates.

all modified DNAzymes was also markedly increased, by approximately 12.5-fold, compared to the unmodified DNAzyme. Among the variants, DNAzyme 3′ AA exhibited the highest substrate conversion rate from $ABTS^{2-}$ to $ABTS^{\bullet+}$. Additionally, the overall catalytic efficiencies (k_{cat}/K_m) of all modified DNAzymes were superior to that of the unmodified counterpart. Both DNAzyme 3′ AA and DNAzyme 3′ AAA exhibit nearly a two-fold increase in catalytic efficiency compared with the unmodified DNAzyme, while DNAzyme 3′A demonstrates an approximately three-fold improvement. Although all three 3′-end adenine modifications lead to similar increases in v_{max} and k_{cat} values, their catalytic efficiencies are not identical. This difference arises because DNAzyme 3′ A possesses a lower K_m value than the other two modified DNAzymes.

Notably, DNAzyme 3′ A showed the highest catalytic efficiency, with a k_{cat}/K_m value of $158.51 \pm 25.05\,s^{-1}\cdot mM^{-1}$—approximately three times greater than the unmodified DNAzyme. These results underscore the significant role of 3′-end A modifications in enhancing the catalytic performance of G-quadruplex/hemin DNAzymes, primarily by increasing turnover rates without compromising structural integrity or requiring enhanced substrate binding[31].

Next, the initial velocity (v_o) of G-quadruplex/hemin DNAzymes (2.5 nM) was measured across a range of H_2O_2 concentrations (5–700 mM), while maintaining a constant ABTS concentration of 2.0 mM. The corresponding Michaelis–Menten plots for each DNAzyme variant are presented in Fig. 6A–D. Kinetic parameters were determined using KaleidaGraph software based on triplicate measurements (with individual data shown in Figure S5), and are summarized in Fig. 6E. Consistent with earlier results, the modified DNAzymes exhibited a significant increase in v_{max}, with values approximately sevenfold higher than that of the unmodified DNAzyme. Interestingly, while most modified variants showed K_m values similar to the unmodified DNAzyme, the DNAzyme with a 3′ AA modification displayed a markedly reduced K_m—approximately 1.6-fold lower. This decrease suggests that the 3′ AA modification enhances the DNAzyme's affinity for H_2O_2, allowing it to reach maximum velocity at lower substrate concentrations. All modified DNAzymes demonstrated elevated turnover numbers (k_{cat}) compared to the unmodified version. Specifically, DNAzyme 3′ A, DNAzyme 3′ AA, and DNAzyme 3′ AAA showed k_{cat} increases of approximately eightfold, sixfold, and 6.8-fold, respectively. Furthermore, the catalytic efficiencies (k_{cat}/K_m) of all modified DNAzymes were significantly higher than that of the unmodified DNAzyme. Among them, DNAzyme 3′ AA exhibited the highest catalytic efficiency, attributed to its combination of enhanced k_{cat} and reduced K_m. These findings underscore the unique advantage of the 3′ AA modification in improving the overall catalytic performance of G-quadruplex/hemin DNAzymes, particularly in terms of substrate affinity and turnover rate.

Previous studies have established that the catalytic cycle of G-quadruplex/hemin DNAzymes involves multiple steps, with the rate-limiting step being the initial reaction of H_2O_2 with hemin to form a highly reactive porphyrin-hydrogen peroxide radical cation intermediate[16,31,32,42]. The kinetic data presented herein highlight the pivotal role of H_2O_2 concentration in governing the overall reaction rate. Given that the DNAzyme with a 3′ AA modification exhibited the highest catalytic efficiency (k_{cat}/K_m) under varying H_2O_2 concentrations, this variant was selected for further evaluation as a signal transducer in a colorimetric biosensor for circulating tumor DNA (ctDNA) detection. ctDNA—fragments of DNA released from tumor cells into the bloodstream—has emerged as a promising biomarker for liquid biopsy-based cancer diagnostics[43,44]. Multiple technologies, including quantitative PCR (qPCR), digital PCR, targeted deep sequencing, and whole-genome sequencing, have been developed for ctDNA detection, offering valuable potential for early cancer diagnosis[45,46]. Among these, biosensors stand out for their versatility and user-friendly platforms. While highly sensitive techniques such as electrochemical, surface-enhanced Raman scattering (SERS), and fluorescence-based biosensors have demonstrated excellent performance in ctDNA analysis[43], they often require sophisticated instruments, expensive reagents, and skilled personnel. In contrast, colorimetric biosensors—relying on visible color changes

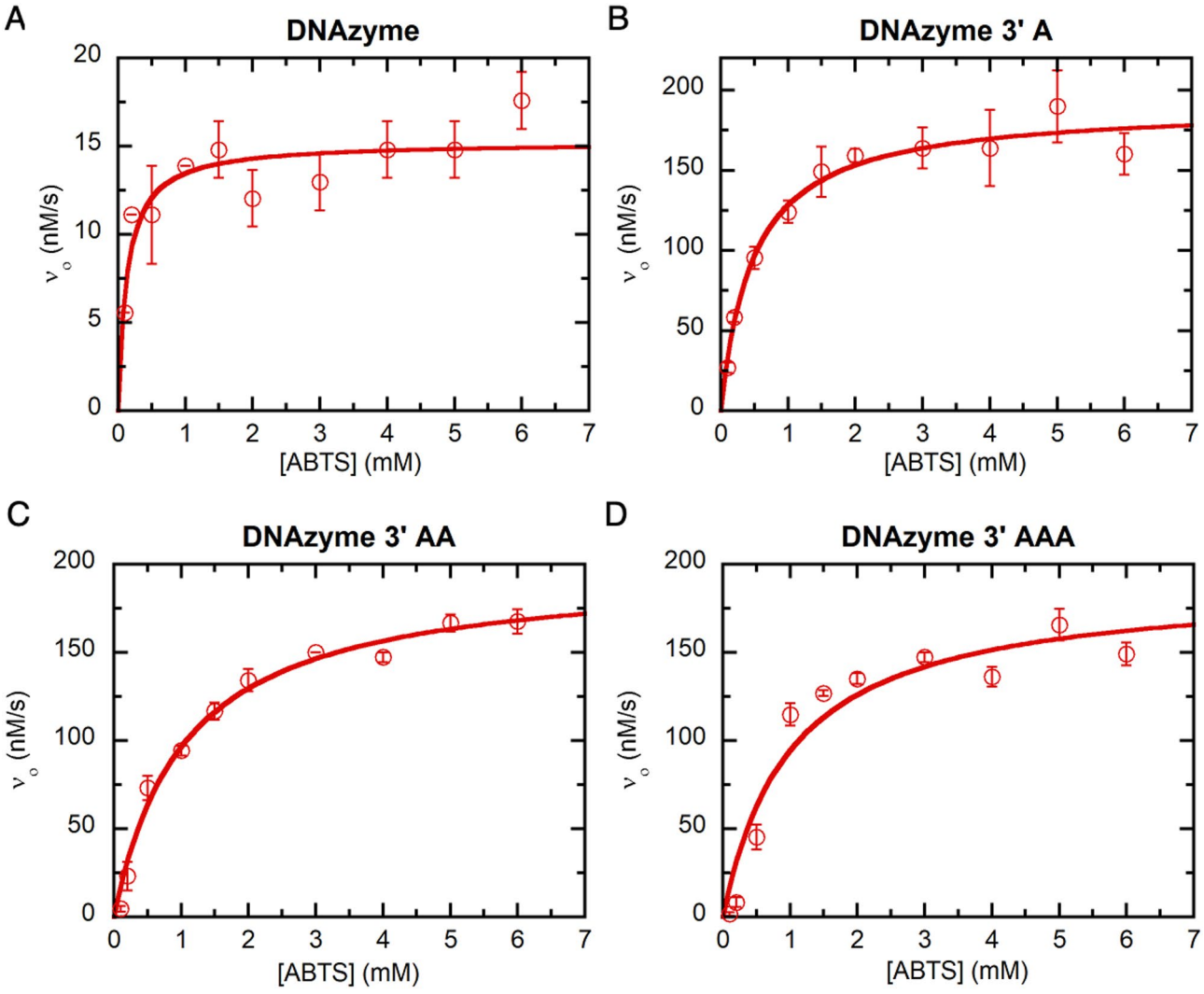

E

	V_{max} (nM/s)	K_m (mM)	k_{cat} (s^{-1})	k_{cat}/K_m (s^{-1}·mM^{-1})
DNAzyme	15.24 ± 0.45	0.13 ± 0.01	6.09 ± 0.18	46.64 ± 3.04
DNAzyme 3' A	190.97 ± 12.37	0.49 ± 0.11	76.39 ± 4.95	158.51 ± 25.02
DNAzyme 3' AA	197.77 ± 3.24	1.05 ± 0.11	79.11 ± 1.29	75.71 ± 7.31
DNAzyme 3' AAA	190.03 ± 6.83	1.02 ± 0.14	75.71 ± 7.31	75.53 ± 8.06

*Conditions: 0.1-6.0 mM ABTS, 300 mM H_2O_2, 2.5 nM DNAzyme

Fig. 5. The Michaelis–Menten plot of DNAzyme (**A**), DNAzyme 3′ A (**B**), DNAzyme 3′ AA (**C**), and DNAzyme 3′ AAA (**D**) with varied ABTS concentrations at 300 mM H_2O_2 concentration and kinetics parameters (**E**). Data presented ± S.D.

upon target recognition—are gaining traction for their simplicity, cost-effectiveness, and potential for point-of-care applications[47–49]. G-quadruplex/hemin DNAzymes are frequently employed as catalytic signal transducers in colorimetric biosensors due to their ability to catalyze peroxidase-like reactions[6,7,50–54]. Enhancing the catalytic activity of DNAzymes offers a direct route to improving biosensor sensitivity. In this study, we designed a colorimetric biosensor for ctDNA detection utilizing G-quadruplex/hemin DNAzymes as the signal transduction element (Fig. 7A). The ctDNA target sequence used in this study is derived from the *KRAS* gene. This gene was selected as a model target because *KRAS* mutations are commonly found in various types of cancer, including pancreatic, colorectal, and lung cancers[55,56]. The biosensor setup involved immobilizing a biotinylated Capture strand (blue) onto agarose beads via streptavidin–biotin binding. The Capture strand was designed to hybridize with one segment of the ctDNA target (red), while the other half of the target sequence hybridized

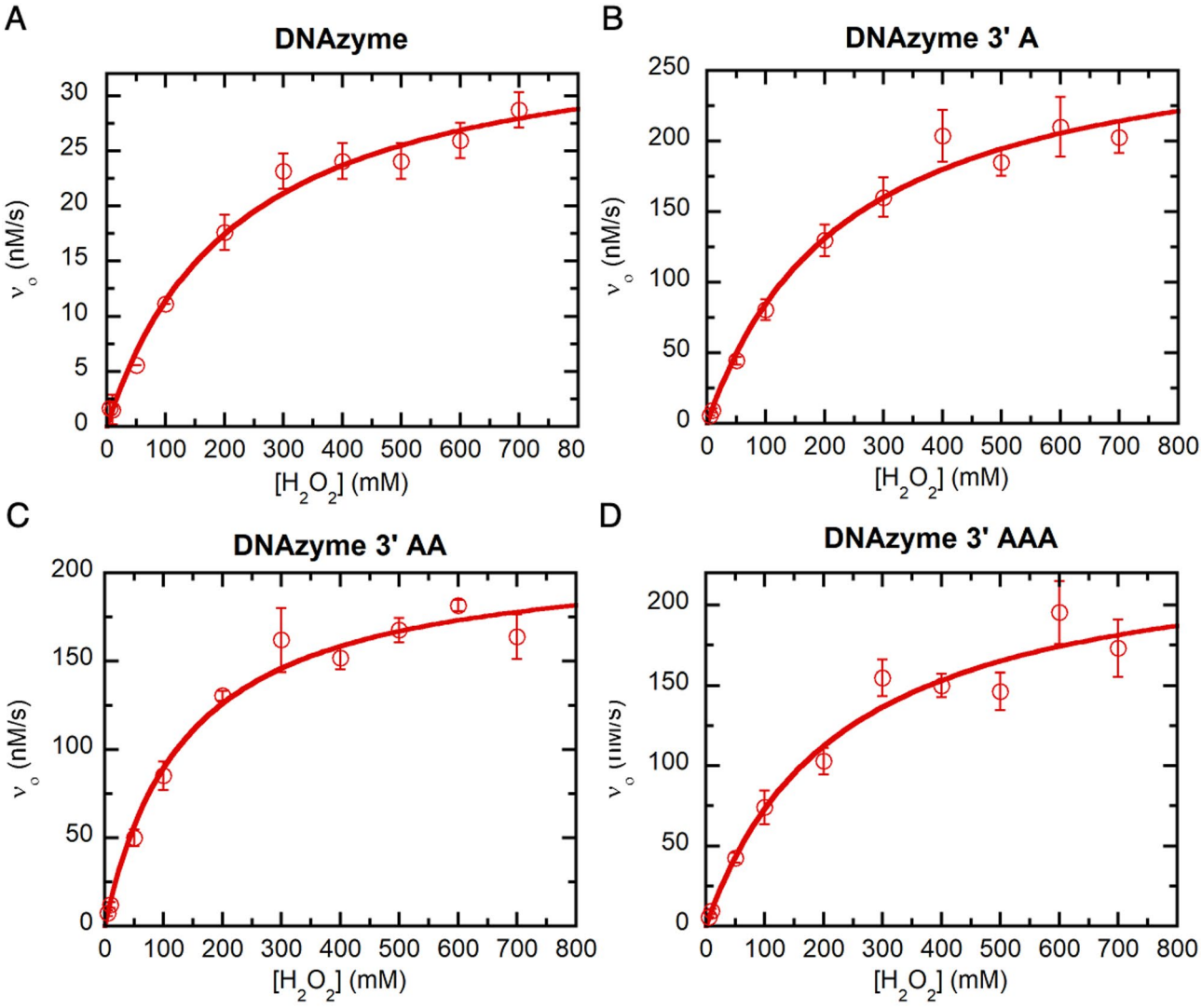

E

	V_{max} (nM/s)	K_m (mM)	k_{cat} (s^{-1})	k_{cat}/K_m (s^{-1}·mM^{-1})
DNAzyme	36.85 ± 2.91	221.68 ± 25.34	14.74 ± 1.16	0.07 ± 0.00
DNAzyme 3' A	291.33 ± 31.05	247.89 ± 70.21	116.53 ± 12.42	0.49 ± 0.08
DNAzyme 3' AA	212.85 ± 7.75	137.28 ± 7.07	85.14 ± 3.10	0.62 ± 0.04
DNAzyme 3' AAA	242.03 ± 18.02	231.83 ± 29.56	96.81 ± 7.21	0.42 ± 0.02

*Conditions: 5-700 mM H_2O_2, 2.0 mM ABTS, 2.5 nM DNAzyme

Fig. 6. The Michaelis–Menten plot of DNAzyme (**A**), DNAzyme 3′ A (**B**), DNAzyme 3′ AA (**C**), and DNAzyme 3′ AAA (**D**) with varied H_2O_2 concentrations at 2.0 mM ABTS concentration and kinetics parameters (**E**). Data presented ± S.D.

with a Signal strand carrying the G-quadruplex/hemin DNAzyme (grey). In the presence of ctDNA, the Signal strand becomes anchored to the bead surface via hybridization, allowing the DNAzyme to catalyze a substrate oxidation reaction and generate a visible green color. In contrast, in the absence of ctDNA, no hybridization or signal generation occurs. To assess the improvement in biosensor performance, both unmodified DNAzyme and 3′ AA-modified DNAzyme were incorporated into the Signal strand by appending a 5′ extension containing a target-complementary sequence (red), resulting in constructs termed Signal and Signal 3′ AA, respectively. This experimental configuration enabled a direct comparison of the catalytic activity and detection sensitivity of the DNAzyme variants within a practical biosensing platform.

The immobilization efficiency of the biotinylated Capture strand on agarose beads was determined to be 79.44%, as calculated from the absorbance at 260 nm of the Capture strand solution before and after the

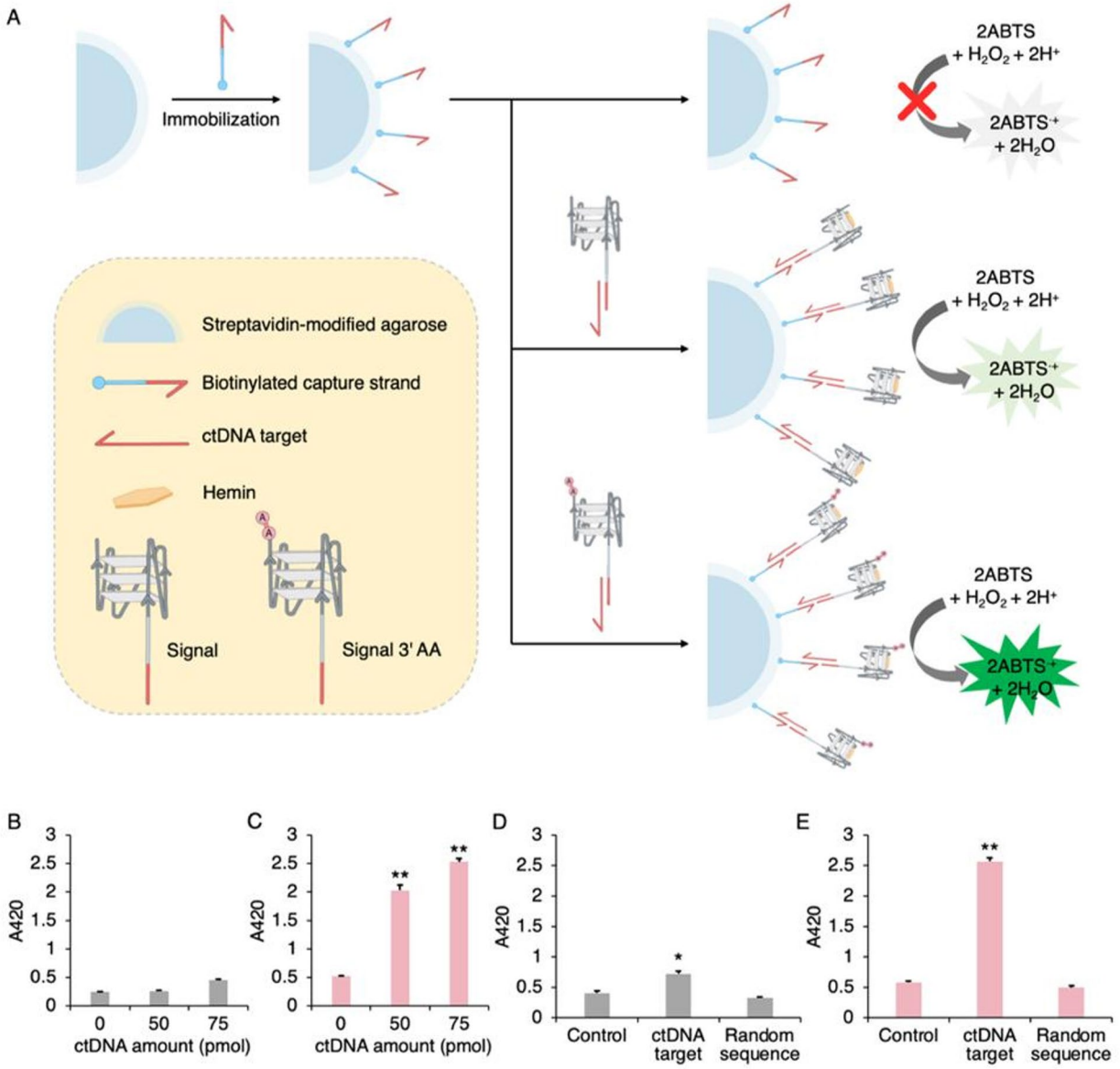

Fig. 7. Schematic representation of the colorimetric ctDNA detection based on G-quadruplex/hemin DNAzyme (**A**). In the absence of the ctDNA target, no color change is observed after substrate addition. In the presence of ctDNA target, DNAzyme in the Signal catalyzes the reaction producing a green-colored solution. The darker green signal could be observed with the Signal 3' AA compared to the Signal. The colorimetric detection of ctDNA target. Signal with different amounts of ctDNA target (**B**), Signal 3' AA with different amounts of ctDNA target (**C**), Signal with ctDNA target and random sequence (**D**), and Signal 3' AA with ctDNA target and random sequence (**E**). Data presented ± S.D. * *P* value < 0.01, ** *P* value < 0.001.

immobilization process (Figure S6). To ensure functional integration into the biosensor system, the catalytic activities of the Signal and Signal 3′ AA constructs were compared with those of the corresponding DNAzyme and DNAzyme 3′ AA controls. The results confirmed that both Signal and Signal 3′ AA retained catalytic activities comparable to their respective free DNAzymes (Figure S7). According to the activity assay, the unmodified DNAzyme exhibited substantially lower catalytic activity than the modified DNAzyme 3′ AA. To evaluate their performance in a biosensing context, both DNAzymes were incorporated into the signal transducer component of a colorimetric biosensor by extending their 5′ ends with sequences complementary to the target. The resulting constructs—Signal (unmodified DNAzyme) and Signal 3′ AA (modified DNAzyme)—were then assessed for signal generation. As expected, the unmodified construct produced a markedly weaker colorimetric response than the modified construct, consistent with their respective catalytic activities. Additionally, the specificity of hybridization among the single-stranded DNA (ssDNA) components of the biosensor was validated, demonstrating that each ssDNA strand selectively hybridized with its intended complementary sequence (Figures S8–S9). As a proof of concept, the biosensor's ability to detect varying concentrations of ctDNA was evaluated. The ctDNA target at concentrations of 0, 25, 50, 75, 100, and 125 pmol was incubated with a fixed

amount (150 pmol) of either Signal or Signal 3′ AA prior to interaction with the immobilized Capture strand. Following a washing step to remove unbound components, ABTS and H_2O_2 substrates were added, and the absorbance at 420 nm (A_{420}) was measured after 10 min of incubation at room temperature. As expected, the system incorporating Signal 3′AA displayed a pronounced increase in the colorimetric signal at A420 with rising ctDNA concentrations, whereas the system with Signal exhibited only a slight increase (full-range sensogram shown in Figure S10). For Signal 3′AA, however, the A420 values approached saturation at higher ctDNA concentrations (100–125 pmol), likely due to the limited amount of Capture-functionalized agarose beads. For the unmodified Signal construct, a slight increase in A_{420} was observed with increasing ctDNA concentrations; however, the difference between 0 and 50 pmol ctDNA was minimal and difficult to distinguish (Fig. 7B). In contrast, the Signal 3′ AA construct exhibited a markedly enhanced A_{420} response with increasing ctDNA concentrations, enabling clear differentiation even at lower target levels (Figs. 7C). Furthermore, the visible color change associated with Signal 3′ AA was significantly more pronounced, underscoring the improved catalytic performance of the 3′ AA-modified G-quadruplex/hemin DNAzyme and its contribution to increased biosensor sensitivity. To further assess the biosensor's specificity, a 75 pmol random DNA sequence was used as a negative control. For comparison, a random DNA sequence with a GC content similar to that of the KRAS target was used. Matching the GC content provides a more appropriate control by minimizing differences in hybridization behavior and structural stability. The results showed that Signal 3′ AA generated a distinct colorimetric signal in response to the ctDNA target, whereas no significant color change was observed with the random sequence. In Fig. 7D,E, the "control" condition refers to reactions without a single-stranded DNA (ssDNA) target, while the "random" condition refers to reactions with a non-specific ssDNA sequence. These findings further confirm the high specificity and superior catalytic activity of Signal 3′AA, underscoring its potential for sensitive and selective ctDNA detection.

Because phosphate-buffered saline (PBS) is widely used in biological experiments due to its physiological compatibility, we also compared different buffer systems commonly applied to G-quadruplex/hemin DNAzymes, including Tris–HCl, MES, HEPES, and PBS. Our results revealed that annealing the G-quadruplex/hemin DNAzyme in Tris–HCl buffer and conducting the catalytic assay in MES buffer yielded the highest catalytic efficiency. Although MES is not typically used in biological systems, its application in our biosensor is feasible. If necessary, DNA molecules can be precipitated and isolated from biological samples prior to analysis, enabling effective use of the biosensor under MES buffer conditions.

In summary, this work provides fundamental insights into the role of flanking nucleotide modifications, highlighting the influence of a 3′ adenine extension on the kinetic behavior of G-quadruplex/hemin DNAzymes. The enhanced catalytic performance of the 3′ AA-modified DNAzyme was further demonstrated by the improved sensitivity of ctDNA detection in a colorimetric biosensor. These results advance our understanding of DNAzyme kinetics and may guide the rational design of DNAzyme-based catalysts with peroxidase activities approaching those of natural HRP enzymes. The catalytically enhanced G-quadruplex/hemin DNAzyme thus represents a promising candidate for applications ranging from biomolecular assays to industrial catalysis.

Conclusions

In this study, the catalytic activities of G-quadruplex/hemin DNAzymes modified with flanking nucleotides at the 3′ and 5′ ends were systematically evaluated using ABTS and H_2O_2 as substrates. Among the tested nucleotide modifications, adenine (A) conferred the most significant catalytic enhancement, while cytosine (C) yielded moderate improvements. In contrast, modifications with thymine (T) or guanine (G) had negligible effects on catalytic activity. Notably, modifications at the 3′ end proved more effective than those at the 5′ end in enhancing catalytic performance. Furthermore, increasing the number of flanking A nucleotides from one to three at the 3′ end did not produce substantial differences, suggesting a plateau in the enhancement effect beyond a single A addition. Circular dichroism (CD) spectroscopy confirmed that all G-rich sequences retained the ability to adopt parallel G-quadruplex structures in the presence of hemin, even with AA modifications at the 3′ end. Kinetic analyses demonstrated that 3′ A-modified DNAzymes exhibited significantly enhanced catalytic turnover rates (k_{cat}), although this modification did not improve substrate binding affinity (K_m). Among the variants, the DNAzyme with a 3′ AA modification achieved the highest catalytic efficiency, particularly when H_2O_2—the rate-limiting substrate in the reaction—was varied. As a proof of concept, we applied this optimized DNAzyme in a colorimetric biosensor for circulating tumor DNA (ctDNA) detection. The enhanced catalytic activity of the 3′ AA-modified DNAzyme translated into markedly improved signal output and sensitivity, enabling reliable detection at low target concentrations. These findings demonstrate that strategic 3′ end modifications can significantly enhance the catalytic performance of G-quadruplex/hemin DNAzymes and hold promise for advancing their application in sensitive biosensing platforms and other DNAzyme-based technologies.

Experimental section

Materials

Single-stranded oligonucleotides and modified oligonucleotides (sequences listed in Table S1) were purchased from Integrated DNA Technologies Pte. Ltd. Tris was obtained from Omnipur (China), while hydrochloric acid (HCl), sodium hydroxide (NaOH), 2-(N-morpholino)ethanesulfonic acid (MES), potassium chloride (KCl), sodium chloride (NaCl), Triton X-100, dimethylsulfoxide (DMSO), hemin, and 2,2′-azino-bis(3-ethylbenzothiazoline-6-sulfonic acid) (ABTS) were procured from Sigma-Aldrich (Canada). Hydrogen peroxide (H_2O_2) was purchased from Merck (Germany), sodium dihydrogen phosphate (NaH_2PO_4) from Qrec (New Zealand), and streptavidin-modified agarose beads from Thermo Fisher Scientific.

Methods

Preparation of G-quadruplex/Hemin DNAzyme

Single-stranded DNA (ssDNA) was annealed in 10 mM Tris–HCl buffer (pH 8.0) containing 50 mM KCl by heating at 90 °C for 5 min, followed by cooling to room temperature for 2 h to form the G-quadruplex structure. The mixture was then incubated with hemin in MES buffer (25 mM MES, pH 5.1, containing 200 mM NaCl, 10 mM KCl, 1% DMSO, and 0.05% Triton X-100) for 30 min.

Examination of catalytic activity

The catalytic activity of the G-quadruplex/hemin DNAzyme was assessed by preparing the DNAzyme as described above and adding ABTS and H_2O_2 substrates to the solution. The mixture was incubated at room temperature for 40 min, and the absorbance was recorded at 420 nm.

Optimization of catalytic activity

KCl dependence. Annealing was performed in 10 mM Tris–HCl buffer (pH 8.0) with or without 50 mM KCl. DNAzyme preparation, substrate addition, and activity measurement followed the same procedure as described above. *Hemin Ratios*. Hemin concentrations were varied, using DNAzyme-to-hemin ratios ranging from 1:1 to 1:50. DNAzyme activity was evaluated under standard conditions. *Annealing Time*. Annealing times were varied from 0 min to overnight. DNAzyme preparation and activity measurement were performed as described. *Hemin Incubation Time*. The hemin incubation time was varied from 0 min to overnight, followed by activity evaluation.

UV–Vis spectrophotometry analysis

The binding complex of the G-quadruplex and hemin was analyzed using a SHIMADZU UV-2501PC spectrophotometer. Hemin (1 μM) was prepared in 10 mM Tris–HCl buffer (pH 8.0), and its absorption spectrum was first recorded. Subsequently, the G-quadruplex strand (1 μM) was added to the hemin solution, and the mixture was incubated at room temperature for 10 min prior to measuring the absorption spectrum.

Circular dichroism (CD) analysis

The conformational changes of G-quadruplex structures with or without hemin were analyzed using a JASCO J-815 CD spectrometer. Samples were prepared at 3 μM in 10 mM Tris–HCl buffer (pH 8.0) and measured in a 0.1 cm path-length cuvette. CD spectra were recorded from 225 to 325 nm at 0.2 nm intervals, with data averaged over three scans.

Kinetic measurements

Kinetic measurements were performed in MES buffer (25 mM MES, pH 5.1) containing 200 mM NaCl, 10 mM KCl, 1% DMSO, and 0.05% Triton X-100, using 2.5 nM DNAzyme. For ABTS kinetic studies, ABTS concentrations ranged from 0.1 to 6.0 mM, while the H_2O_2 concentration was fixed at 300 mM. For H_2O_2 kinetic studies, H_2O_2 concentrations ranged from 5 to 700 mM, with ABTS fixed at 2.0 mM. The oxidation of $ABTS^{2-}$ to $ABTS^{\bullet+}$ was monitored by measuring absorbance at 420 nm every 15 s over a 2-min period. The molar extinction coefficient of $ABTS^{\bullet+}$ at 420 nm (ε_{420}) was 36,000 M^{-1} cm^{-1} [31,57]. Kinetic parameters (v_{max}, K_m, and k_{cat}) were determined using KaleidaGraph software (version 4.0) via nonlinear regression analysis with the Marquardt–Levenberg algorithm.

Immobilization of biotinylated ssDNA on streptavidin-modified beads

Biotinylated capture strands were prepared in PBS buffer (0.1 M phosphate, 0.15 M NaCl, pH 7.2) and denatured by heating at 90 °C for 5 min. Streptavidin-modified agarose beads were washed with PBS (pH 7.2) and incubated with the capture strand at room temperature for 3 h with gentle shaking. The beads were then washed three times with PBS and stored at 4 °C for further experiments. Absorbance at 260 nm was measured to calculate immobilization efficiency.

Interaction of ssDNA components

Interactions between ssDNA components were examined by annealing in 10 mM Tris–HCl buffer (pH 8.0) at 90 °C for 5 min, followed by cooling to room temperature for 30 min. Samples were analyzed using 12% polyacrylamide gel electrophoresis (PAGE) at 4 °C.

Colorimetric detection of ctDNA target

For ctDNA detection, the ctDNA target (0, 25, 50, 75, 100, and 125 pmol) and Signal strand (150 pmol; either Signal or Signal 3' AA) were annealed in PBS (pH 7.2) by heating at 90 °C and cooling to room temperature for 30 min. The annealed complexes were incubated with capture-functionalized agarose beads, followed by washing with PBS (pH 7.2). Hemin in MES buffer (pH 5.1) was added, and the mixture was incubated at room temperature for 30 min. ABTS (20 mM) and H_2O_2 (25 mM) were then added, and the absorbance at 420 nm was recorded after 10 min. For specificity assays, random ssDNA (75 pmol) was used in place of the ctDNA target. All steps followed the same protocol as described above.

Data availability

The datasets used and/or analyzed during the current study available from the corresponding author on reasonable request.

Received: 6 June 2025; Accepted: 10 October 2025

Published online: 17 November 2025

References

1. Liu, J., Cao, Z. & Lu, Y. Functional nucleic acid sensors. *Chem. Rev.* **109**, 1948–1998 (2009).
2. Wang, Y., Nguyen, K., Spitale, R. C. & Chaput, J. C. A biologically stable DNAzyme that efficiently silences gene expression in cells. *Nat. Chem.* **13**, 319–326 (2021).
3. Liao, Y., Guo, S., Hua, X., Yuan, R. & Xu, W. Autocatalytic replicated Mg^{2+}-ligation DNAzyme as robust biocatalyst for sensitive, label-free and enzyme-free electrochemical biosensing of protein. *Sens. Actuators B Chem.* **310**, 127862 (2020).
4. Kohler, T. et al. DNAzymes as catalysts for L-tyrosine and amyloid β oxidation. *ACS Omega* **5**, 7059–7064 (2020).
5. Shumayrikh, N. M., Warren, J. J., Bennet, A. J. & Sen, D. A heme•DNAzyme activated by hydrogen peroxide catalytically oxidizes thioethers by direct oxygen atom transfer rather than by a compound I-like intermediate. *Nucleic Acids Res.* **49**, 1803–1815 (2021).
6. Chen, X. et al. A universal probe design for colorimetric detection of single-nucleotide variation with visible readout and high specificity. *Sci. Rep.* **6**, 20257 (2016).
7. Long, Y. et al. Ultrasensitive visual detection of HIV DNA biomarkers via a multi-amplification nanoplatform. *Sci. Rep.* **6**, 23949 (2016).
8. Liang, G. et al. Chemiluminescence assay for detection of 2-hydroxyfluorene using the G-quadruplex DNAzyme-H_2O_2-luminol system. *Microchim. Acta* **185**, 54 (2018).
9. Wang, L. et al. Sensitive and label-free electrochemical lead ion biosensor based on a DNAzyme triggered G-quadruplex/hemin conformation. *Biosens. Bioelectron.* **115**, 91–96 (2018).
10. Travascio, P., Li, Y. & Sen, D. DNA-enhanced peroxidase activity of a DNA aptamer-hemin complex. *Chem. Biol.* **5**, 505–517 (1998).
11. Chang, T. et al. Activity enhancement of G-quadruplex/hemin DNAzyme by flanking d(CCC). *Chem. Eur. J.* **22**, 4015–4021 (2016).
12. Li, J. et al. Zippered G-quadruplex/hemin DNAzyme: Exceptional catalyst for universal bioanalytical applications. *Nucleic Acids Res.* **49**, 13031–13044 (2021).
13. Zhang, J. et al. A novel Tb3+-promoted G-quadruplex-hemin DNAzyme for the development of label-free visual biosensors. *Biosens. Bioelectron.* **26**, 4053–4057 (2011).
14. Nakayama, S. & Sintim, H. O. Investigating the interactions between cations, peroxidation substrates and G-quadruplex topology in DNAzyme peroxidation reactions using statistical testing. *Anal. Chim. Acta* **747**, 1–6 (2012).
15. Golub, E., Freeman, R. & Willner, I. A hemin/G-quadruplex acts as an NADH oxidase and NADH peroxidase mimicking DNAzyme. *Angew. Chem. Int. Ed.* **50**, 11710–11714 (2011).
16. Cao, Y. et al. Investigation and improvement of catalytic activity of G-quadruplex/hemin DNAzymes using designed terminal G-tetrads with deoxyadenosine caps. *Chem. Sci.* **11**, 6896–6906 (2020).
17. Xiao, Y., Pavlov, V., Gill, R., Bourenko, T. & Willner, I. Lighting up biochemiluminescence by the surface self-assembly of DNA-hemin complexes. *ChemBioChem* **5**, 374–379 (2004).
18. Liu, G., Yuan, Y. & Wang, J. Hemin/G-quadruplex DNAzyme nanowires amplified luminol electrochemiluminescence system and its application in sensing silver ions. *RSC Adv.* **6**, 37221–37225 (2016).
19. Yang, X. et al. Characterization of G-quadruplex/hemin peroxidase: substrate specificity and inactivation kinetics. *Chem. Eur. J.* **17**, 14475–14484 (2011).
20. Golub, E., Freeman, R., Niazov, A. & Willner, I. Hemin/G-quadruplexes as DNAzymes for the fluorescent detection of DNA, aptamer-thrombin complexes, and probing the activity of glucose oxidase. *Analyst* **136**, 4397–4401 (2011).
21. Kosman, J., Zukowski, K., Csaki, A., Fritzsche, W. & Juskowiak, B. Sequence effect on the activity of DNAzyme with covalently attached hemin and their potential bioanalytical application. *Sensors* **22**, 500 (2022).
22. Kong, D.-M. Factors influencing the performance of G-quadruplex DNAzyme-based sensors. *Methods* **64**, 199–204 (2013).
23. Golub, E., Albada, H. B., Liao, W.-C., Biniuri, Y. & Willner, I. Nucleoapzymes: Hemin/G-quadruplex DNAzyme-aptamer binding site conjugates with superior enzyme-like catalytic functions. *J. Am. Chem. Soc.* **138**, 164–172 (2016).
24. Kosman, J., Stanislawska, A., Gluszynska, A. & Juskowiak, B. Conjugation of hemin to G-quadruplex forming oligonucleotide using click chemistry. *Int. J. Biol. Macromol.* **101**, 799–804 (2017).
25. Kosman, J., Zukowski, K. & Juskowiak, B. Comparison of characteristics and DNAzyme activity of G4-hemin conjugates obtained via two hemin attachment methods. *Molecules* **23**, 1400 (2018).
26. Zhang, Y., Ma, J., Luo, F., Wang, W. & Cui, X. Design of a high-sensitivity dimeric G-quadruplex/hemin DNAzyme biosensor for norovirus detection. *Molecules* **26**, 7352 (2021).
27. Adeoye, R. I. et al. Catalytic activities of multimeric G-quadruplex DNAzymes. *Catalysts* **9**, 613 (2019).
28. Kong, D.-M., Xu, J. & Shen, H.-X. Positive effects of ATP on a G-quadruplex-hemin DNAzyme-mediated reactions. *Anal. Chem.* **82**, 6148–6153 (2010).
29. Qi, C. et al. Activity enhancement of G-quadruplex/hemin DNAzyme by spermine. *RSC Adv.* **4**, 1441 (2014).
30. Qiu, D. et al. Effect of distance from catalytic synergy group to iron porphyrin center on activity of G-quadruplex/hemin DNAzyme. *Molecules* **25**, 3425 (2020).
31. Li, W. et al. Insight into G-quadruplex-hemin DNAzyme/RNAzyme: Adjacent adenine as the intramolecular species for remarkable enhancement of enzymatic activity. *Nucleic Acids Res.* **44**, 7373–7384 (2016).
32. Guo, Y. et al. A thermophilic tetramolecular G-quadruplex/hemin DNAzyme. *Angew. Chem. Int. Ed.* **56**, 16636–16640 (2017).
33. Virgilio, A., Esposito, V., Lejault, P., Monchaud, D. & Galeone, A. Improved performances of catalytic G-quadruplexes (G4-DNAzymes) via the chemical modifications of the DNA backbone to provide G-quadruplexes with double 3'-external G-quartets. *Int. J. Biol. Macromol.* **151**, 976–983 (2020).
34. Chen, J., Guo, Y., Zhou, J. & Ju, H. The effect of adenine repeats on G-quadruplex/hemin peroxidase mimicking DNAzyme activity. *Chemistry* **23**, 4210–4215 (2017).
35. Cheng, M. et al. Relations between the loop transposition of DNA G-quadruplex and the catalytic function of DNAzyme. *Biochim. Biophys. Acta. Gen. Subj.* **1861**, 1913–1920 (2017).
36. Li, T., Dong, S. & Wang, E. G-quadruplex aptamers with peroxidase-like DNAzyme functions: Which is the best and how does it work?. *Chem. Asian. J.* **4**, 918–922 (2009).
37. Nasab, M. G., Hassani, L., Nejad, S. M. & Norouzi, D. Interaction of hemin with quadruplex DNA. *J. Biol. Phys.* **43**, 5–14 (2017).
38. Li, T., Wang, E. & Dong, S. Potassium-lead-switched G-quadruplexes: A new class of DNA logic gates. *J. Am. Chem. Soc.* **131**, 15082–15083 (2009).
39. Wang, Z., Zhao, J. Z., Bao, J. & Dai, Z. Construction of metal-ion-free G-quadruplex-hemin DNAzyme and its application in S1 nuclease detection. *ACS Appl. Mater. Interfaces* **8**, 827–833 (2016).
40. Tang, G., Zhao, C., Gao, J. & Tan, H. Colorimetric detection of hydrogen sulfide based on terbium-G-quadruplex-hemin DNAzyme. *Sens. Actuators B Chem.* **237**, 795–801 (2016).
41. Nakayama, S., Wang, J. & Sintim, H. O. DNA-based peroxidation catalyst—What is the exact role of topology on catalysis and is there a special binding site for catalysis?. *Chem. Eur. J.* **17**, 5691–5698 (2011).
42. Chen, J. et al. A push-pull mechanism helps design highly competent G-quadruplex-DNA catalysts. *CCS Chem.* **2**, 2183–2193 (2020).
43. Li, X. et al. Liquid biopsy of circulating tumor DNA and biosensor applications. *Biosens. Bioelectron.* **126**, 596–607 (2019).

44. Connal, S. et al. Liquid biopsies: The future of cancer early detection. *J. Transl. Med.* **21**, 118 (2023).
45. Zou, Z. et al. Technologies for analysis of circulating tumor DNA: Progress and promise. *Trends Anal. Chem.* **97**, 36–49 (2017).
46. Palmirotta, R. et al. Liquid biopsy of cancer: A multimodal diagnostic tool in clinical oncology. *Ther. Adv. Med. Oncol.* **10**, 1–24 (2018).
47. Pan, B., El-Moghazy, A. Y., Norwood, M., Nitin, N. & Sun, G. Rapid and ultrasensitive colorimetric biosensors for onsite detection of Escherichia coli O157:H7 in fluids. *ACS Sens.* **9**, 912–922 (2024).
48. Liu, B., Zhuang, J. & Wei, G. Recent advances in the design of colorimetric sensors for environmental monitoring. *Environ. Sci. Nano* **7**, 2195–2213 (2020).
49. Zhou, J. et al. Recent advances in design and application of nanomaterials-based colorimetric biosensors for agri-food safety analysis. *ACS Omega* **49**, 46346–46361 (2023).
50. Chen, W. et al. DNA transducer-triggered signal switch for visual colorimetric bioanalysis. *Sci. Rep.* **5**, 11190 (2015).
51. Zhang, H., Li, X., He, F., Zhao, M. & Ling, L. Turn-off colorimetric sensor for sequence-specific recognition of single-stranded DNA based upon Y-shaped DNA structure. *Sci. Rep.* **8**, 12021 (2018).
52. Batule, B. S. et al. Colorimetric detection of norovirus in oyster samples through DNAzyme as a signaling probe. *J. Agric. Food. Chem.* **66**, 3003–3008 (2018).
53. Chen, J. et al. Highly active G-quadruplex/hemin DNAzyme for sensitive colorimetric determination of lead(II). *Microchim. Acta.* **186**, 786 (2019).
54. Chen, Y. et al. Highly sensitive biosensing applications of a magnetically immobilizable covalent G-quadruplex/hemin DNAzyme catalytic system. *Anal. Chem.* **94**, 2212–2219 (2022).
55. Lee, K.-Y. et al. Oncogenic KRAS G12D mutation promotes dimerization through a second, phosphatidylserine-dependent interface: A model for KRAS oligomerization. *Chem. Sci.* **12**, 12827–12837 (2021).
56. Yang, Y., Zhang, H., Huang, S. & Chu, Q. KRAS mutations in solid tumors: Characteristics, current therapeutic strategy, and potential treatment exploration. *J. Clin. Med.* **12**, 709 (2023).
57. Kenzom, T., Srivastava, P. & Mishra, S. Structural insights into 2,2'-azino-bis(3-ethylbenzothiazoline-6-sulfonic acid) (ABTS)-mediated degradation of reactive blue 21 by engineered *Cyathus bulleri* laccase and characterization of degradation products. *Appl. Environ. Microbiol.* **80**, 7484–7495 (2014).

Acknowledgements

This work was supported by Grant No. RGNS63-141 by the Office of the Permanent Secretary, Ministry of Higher Education, Science, Research and Innovation (OPS MHESI), Thailand Science Research and Innovation (TSRI), Burapha University (A.U.), Mahidol University (T.K., S.C.). We also thank Mahidol University – Frontier Research Facility (MU-FRF) for technical assistance.

Author contributions

S.C. carried out the experiments. A.U. designed and carried out the experiments, analyzed the results, and wrote the manuscript. T.K. designed, supervised the experiments, performed the data analysis, and wrote the manuscript. All authors reviewed the manuscript.

Declarations

Competing interests

The authors declare no competing interests.

Additional information

Supplementary Information The online version contains supplementary material available at https://doi.org/10.1038/s41598-025-24052-1.

Correspondence and requests for materials should be addressed to A.U. or T.K.